Numerical Modeling of a Time Reversal Experiment in Shallow Singapore Waters

H.C. Song, W.S. Hodgkiss, and J.D. Skinner
Marine Physical Laboratory, Scripps Institution of Oceanography
La Jolla, CA 92037-0238, USA

Venugopalan Pallayil, Paul James Seekings, Iulian Topor, and John Robert Potter
Acoustics Research Laboratory, Tropical Marine Science Institute,
National University of Singapore, 12A Kent Ridge Road, Singapore 11923

Abstract **– The Time Reversal Mirror (TRM) technique is a very useful tool in many underwater applications. Its usefulness in reverberation rejection and underwater communications has already been established through experiments by the Marine Physical Laboratory. The design of a TRM experiment is specific to the location and environment where it is being conducted. This paper presents theoretical and numerical analysis of a time reversal experiment which will be conducted in very shallow water (15-20 m depth) in Singapore waters. The objective of the numerical simulation was to arrive at the various design parameters for the experiment and thus to predict its performance. The main parameters under question were the optimum frequencies to be used and the focusing ranges to be investigated. Extensive measurements were carried out at the selected site to obtain information about the ambient noise, time evolving sound speed structure and also the sound velocity in the sea-bed. The bottom sound speed was computed from the bulk density and porosity of the core samples collected from various locations at the site using an empirical formula. Direct measurements were also done to find out the propagation losses at three different frequencies (7.5, 10 and 12.5 kHz) and at three different depths (4, 8 and 12 m) over a 500 m range. A short description of the system hardware also is presented.**

I. INTRODUCTION

Over the last decade, the Time Reversal Mirror (TRM) has been studied extensively in underwater acoustics [1] [2]. Its usefulness in reverberation rejection [3] and underwater communications [4] has already been established through experiments by the Marine Physical Laboratory. The design of a TRM experiment is specific to the location and environment where it is being conducted. This paper presents theoretical and numerical analysis of a time reversal experiment which will be conducted in very shallow water (15-20 m depth) in Singapore waters. The Singapore waters are also interesting because of the non-Gaussian ambient noise due to the presence of snapping shrimp.

The objective of the numerical simulation was to arrive at the various design parameters for the experiment and thus to predict its performance. The main parameters under question were the optimum frequencies to be used and the focusing ranges to be investigated. Extensive measurements were carried out at the selected site to obtain information about the ambient noise, time evolving sound speed structure and also the sound velocity in the sea-bed. The bottom sound speed was computed from the bulk density and porosity of the core samples collected from various locations at the site using an empirical formula. In addition, direct measurements were done to find out the propagation losses at three different frequencies (7.5, 10 and 12.5 kHz) for three different depths (4, 8 and 12 m) over a 500 m range. A description of the hardware is also presented.

II. NUMERICAL MODELING

A. Environmental Model

The acoustic environment was modeled as a Pekeris waveguide as shown in Figure. 1, although the details of the geo-acoustic parameters (sediment sound speed) indicate some range-dependency (1550-1650 m/s) along with bathymetric changes (15-22 m). The vertical TRM array covers the water column from 1 m to 15 m in 18-m water depth with an aperture of $L = 14$ m and inter-element spacing of $\Delta z = 0.5$ m which corresponds to 3.5 times the wavelength at the center frequency of $f = 10$ kHz. The number of TRM elements was $N = 29$.

The sound speed profiles within the water column were measured by CTD casts at the experimental site on January 20, 2004. Over a period of six hours, the profile remained remarkably stable and constant with depth (i.e., iso-speed).

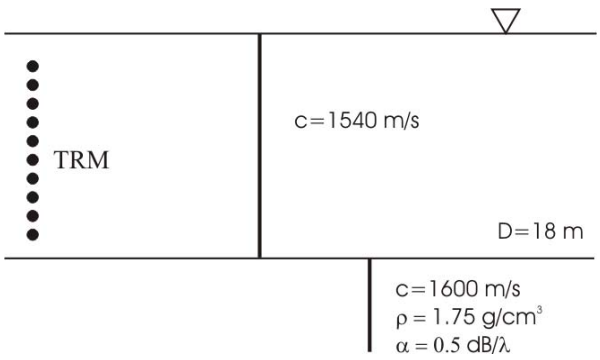

Figure 1. Pekeris waveguide model.

B. Forward Propagation: PS to TRM

Figure. 2 illustrates a schematic of time reversal experiment involving two-way propagation: (1) forward propagation from a probe source (PS) to the TRM and (2) backward propagation from the TRM back to the PS. The Source Receiver Array (SRA) is equivalent to the TRM. Numerical modeling follows these procedures.

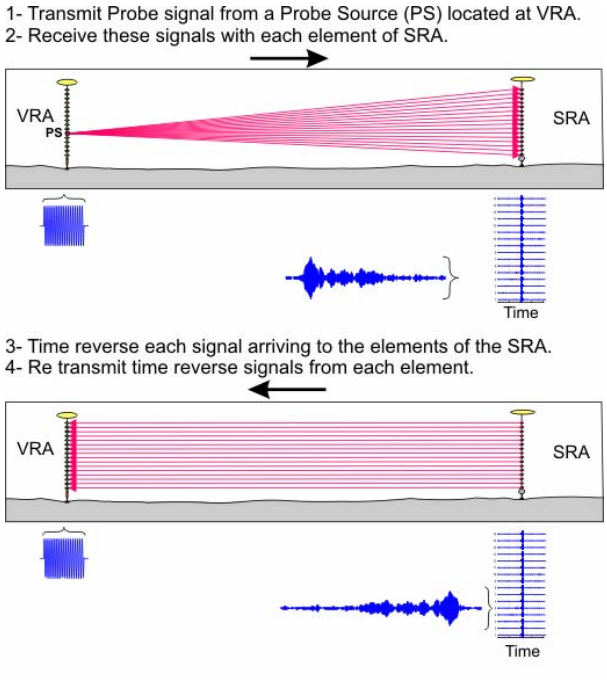

Figure 2. Schematic of a time reversal experiment.

Figure. 3 shows the probe source (PS) ping captured by the TRM array at three different ranges: (a) 0.5 km, (b) 1 km, and (c) 2 km. The PS is at 10 m depth and the PS ping is 0.4 ms CW (continuous wave) tone at 10 kHz with 50% bandwidth. The dispersion characteristics suggest that the TRM array needs to capture the PS ping in about a 50 ms time window.

C. Back propagation: TRM to PS

The PS pings captured (shown in Figure. 3) are time-reversed and retransmitted towards back to the PS for time reversal focusing. Figure. 4 shows the corresponding signal received by a vertical receive array (VRA), which is collocated in range with the PS, to measure the focus. Figure. 4(d) shows the energy over a 3-ms time window as a function of depth at three different ranges.

Referring to figure 4(d), it can be seen that the side-lobe levels at 2 km range (20-25 dB) is lower than the other two at closer ranges (15-20 dB). This is due to the fact that the 29-element TRM array described above under samples the higher order modes contributing at closer ranges, for the given element spacing. The higher order modes, however, contribute less at 2 km range due to significant attenuation at longer range, resulting in better side-lobe suppression. The tight focus along the depth also suggests that a VRA must be positioned around the PS depth with dense sampling.

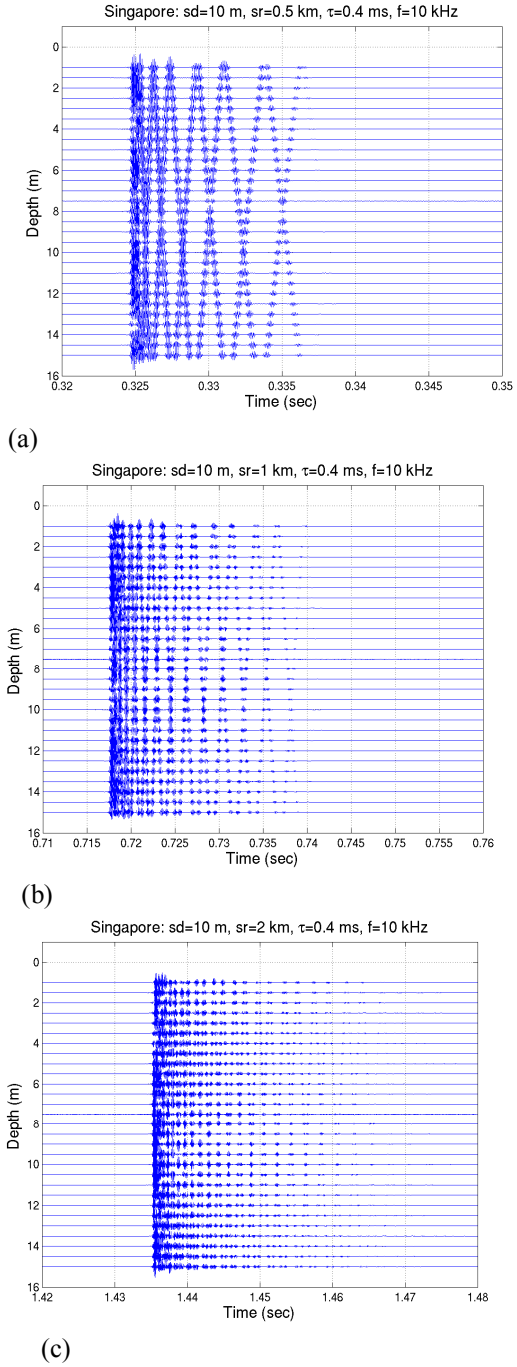

Figure. 3. PS ping captured by the TRM array at three different ranges: (a) 0.5 km, (b) 1 km, and (c) 2 km. Note that the time scales are different.

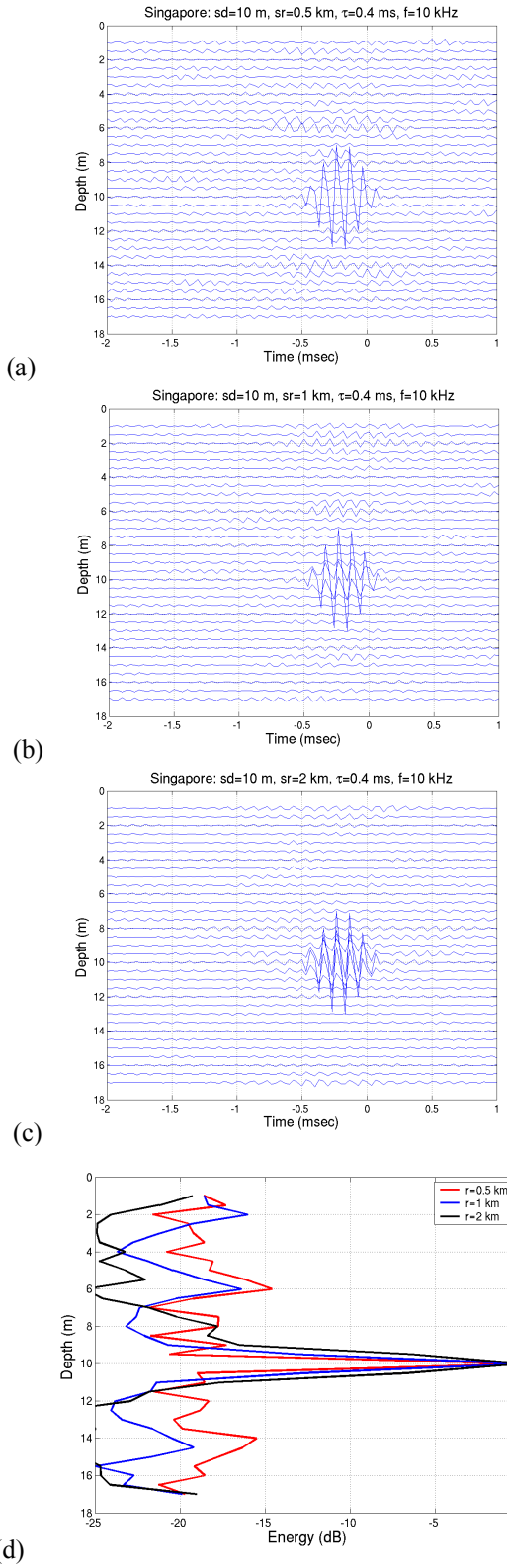

Figure. 4. Panels (a)-(c) show signals received on the VRA from time reversed transmission of pulses shown in Figure. 3 (a)-(c), respectively. Plot (d) shows the energy over a 3-ms time window as a function of depth at three different ranges.

D. Matched Field Processing

The TRM is relevant to the recent trends in acoustic signal processing which have emphasized utilizing the knowledge of the environment, e.g., matched field processing (MFP) [5]. However, MFP requires accurate knowledge of the environment along the propagation path. Phase-conjugation in the frequency domain is an environmentally self-adaptive process that can be applied to localization problems and communications in complicated ocean environments.

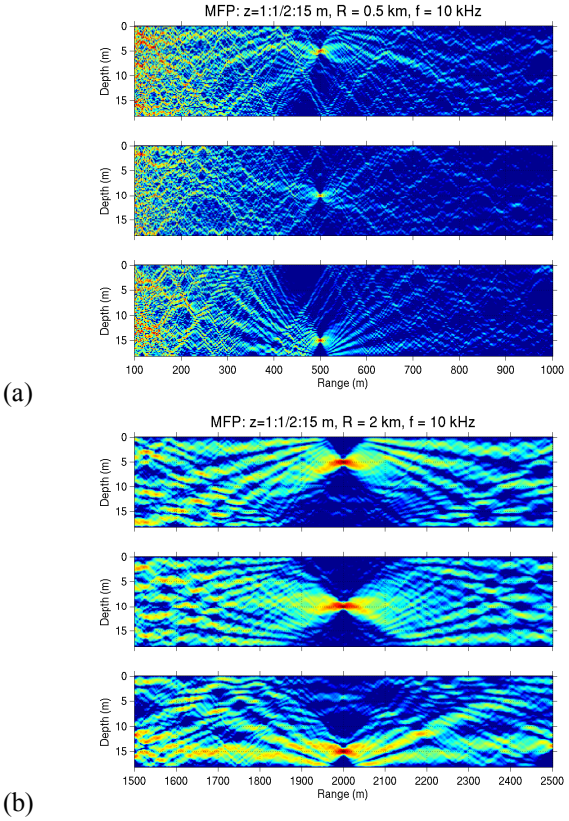

Figure. 5. MFP results for three different PS depths (5-m, 10-m, 15-m) at two different ranges: (a) 0.5 km and (b) 2 km.

Figure. 5 displays MFP ambiguity surfaces for a PS at two different ranges (0.5 km and 2 km) for three different depths (5 m, 10 m, 15 m), showing the focal structures and sizes for a given TRM array configureuration at the center frequency of 10 kHz. With a VRA located at the same range of the PS we can only measure a vertical cut of the ambiguity surface at a single range.

Interestingly, Figure. 6 shows that we can shift the focus in range through an easily-implemented frequency shifting procedure prior to retransmission at the TRM when the PS is at 10 m depth and 1 km range (shown in the middle panel). The top panel shows the focus at 0.9 km range with a center frequency of $f = 9$ kHz while the bottom panel has a focus at 1.1 km range with $f = 11$ kHz. The waveguide invariant theory predicts the range shift of approximately

± 10% over the frequency range where the mode shapes do not change significantly [6].

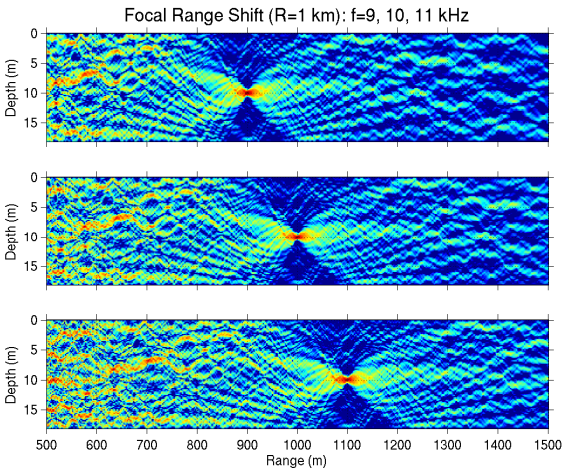

Figure. 6. Focal range shift using an appropriate frequency shift. The original PS is at 15 m depth and 1 km range (middle). The top panel shows the focus shifted at 0.9 km range while the bottom panel has a focus at 1.1 km range.

E. Transmission Loss (TL)

Figure. 7 shows the transmission loss (TL) calculated at the center frequency of $f = 10$ kHz for various sediment sound speeds representing the minimum (1550 m/s), the mean (1600 m/s), and the maximum (1650 m/s). The TL displayed here is an incoherent summation of the modes when both the source and receiver are at 10 m depth. Note that TL is much larger with a bottom speed of 1550 m/s (blue curve) which is close to the sound speed in the water column (1540 m/s) because significant energy is transmitted into the bottom due to a small impedance contrast at the water/bottom interface.

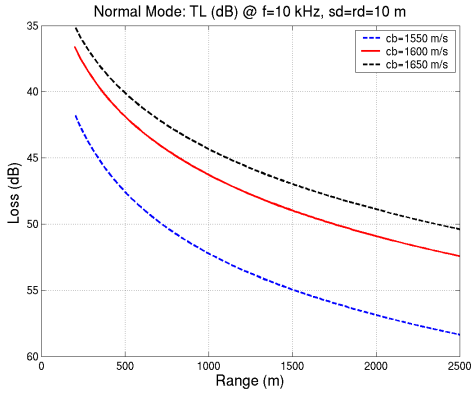

Figure. 7. Transmission loss (TL) for various sediment sound speeds representing the minimum (1550 m/s, blue), the mean (1600 m/s, red), and the maximum (1650 m/s, black). At 1 km range, the TL is between 44-53 dB depending upon the sediment speed.

Figure 8 shows a contour plot of field strength in range (0.2-2 km) and depth (0-18 m) for (a) a single PS transmission and (b) broadside array transmission. A broadside transmission is an excitation of the TRM with equal amplitudes. Since the field is calculated with respect to a source level (SL) of 0 dB at 1 m.

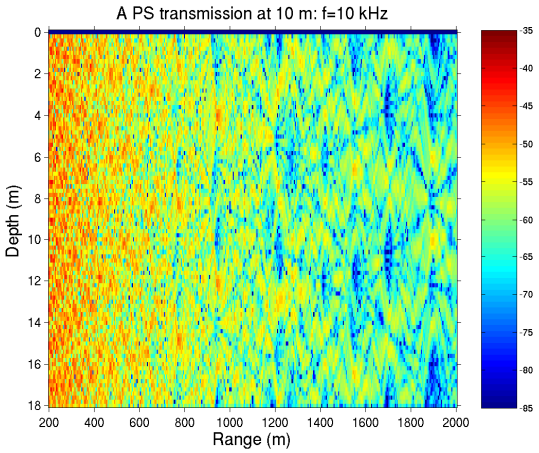

(a)

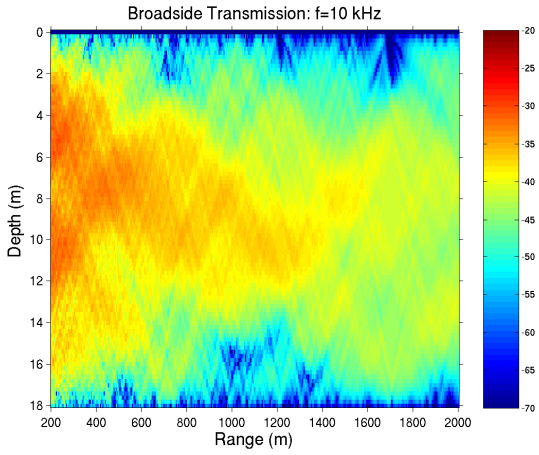

(b)

Figure. 8. The field strength in range and depth. (a) A single PS transmission at 10 m depth. (b) Broadside transmission of the TRM.

F. Thinning of the TRM Array

For practical purposes, it is also interesting to investigate the degradation in focusing with fewer elements than the full set of TRM transducers [7]. Figure. 9(a)-(c) shows back-propagation results produced from various subsets of TRM transducers with $N = 15$ for a PS at 10-m depth and 1 km range: (a) every other element, (b) first half (top), and (c) second half (bottom). The result using the full set ($N = 29$) is shown in Figure. 4(b). Figure. 9(d) displays the energy distribution along the depth, indicating that keeping the aperture of the array (blue) is more important than the inter-element spacing given the number of transducers.

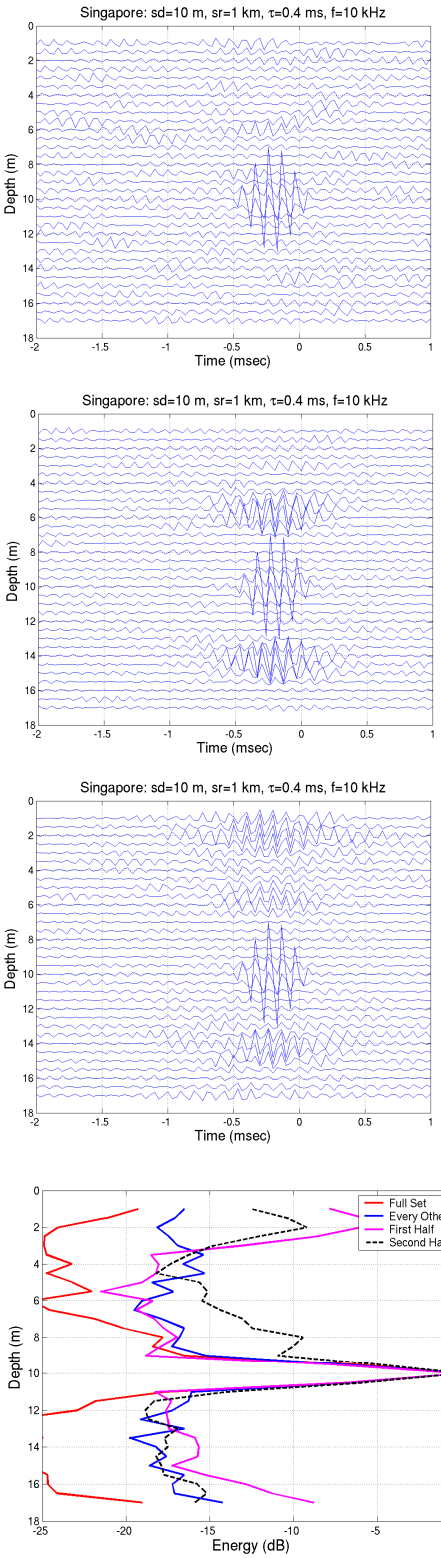

Figure 9. Signals produced from various subsets of TRM transducers when $N = 15$ for a PS at 10 m depth and 1 km range: (a) every other element, (b) first half, and (c) second half. The result using the full set of TRM transducers when $N = 29$ is displayed in Figure. 4(b). (d) displays the energy over a 3 ms time window as a function of depth for various configurations.

III. DESCRIPTION OF HARDWARE

A time reversal mirror (TRM) consisting of 29 source/receive transducers operating in the 7.5-12.5 kHz band is being built. The total SRA array aperture is 14 m with inter-element spacing of 0.5 m which corresponds to 3.5 times the wavelength at the center frequency of 10 kHz. The elements of the SRA employs model no. CTG 0052-1 transducers from Chelsea Technologies Group, UK. Each element has a Transmitting Voltage Response (TVR) of 133 dB re 1 µPa/V @ 10kHz and a receiving sensitivity of -180 ± 1 dB re 1 V/µPa over the band 8 to 13 kHz. Each of the transducer elements can handle a continuous power level of 100W and a pulsed power level of 300W. A 16-element vertical receiver array (VRA) collocated with a probe source (PS) will be deployed at various ranges (0.5-2 km) from the TRM. The VRA is made using SQ026 (see figureure 11) hydrophones from Sensor Technologies, Canada and comes with an integrated preamplifier of 40 dB

Figure 10 A rendering showing the arrangement of a section of the SRA . On top is the transducer element

gain. The overall sensitivity of the receiving element is -153 dB re 1 V/µPa, over the frequency range 100 Hz to 26 kHz. Both the VRA and SRA follow a ladder type construction to avoid any twisting of the array in high currents and also to avoid bunching of the cable onto one side leading to distortions in the beampatterns of the transducers. Figure 10 shows the array arrangement along with the transducer in the inset. The probe source (PS) employs one transducer element similar to the SRA element and a power amplifier. Both the SRA and the PS can generate source levels of about 190 dB re 1 µPa @ 1m which is sufficient to cover the maximum range of 2 km.

The data acquisition system consists of two units, an analog to digital converter (ADC) for acquiring the data from the SRA and digitizing it and a digital to analog converter (DAC) card which regenerates the time reversed analog signals for re-transmission from the SRA to the

VRA. ICS-610-32, a 32 channel ADC manufactured by

Figure 11 SQ026 hydrophone with 40 dB integrated preamplifier

Integrated Circuit Systems, USA and the ICS-625B-32, the corresponding DAC have been selected for our application based on the channel requirements and the sampling frequency. The SRA is normally connected to the receiver and during transmissions the receiver is disabled and the signals are routed to the power amplifier through a Transmit/Receive switch. All the time reversal computations required at the SRA side are performed locally in a PC using MATLAB codes. A 16-channel data acquisition system is used at the VRA side to receive the TRM signals. From the received signals the TRM focus is computed.

The first set of trials is planned from late April, 2006.

IV. SUMMARY

Using a simple Pekeris waveguide model, we investigated theoretically the feasibility of a time reversal experiment using the hardware design above in very shallow water. In the simulation the probe source was placed at 10m depth and a 0.4 ms CW tone at 10 kHz was sent out. The dispersion characteristics suggest that the TRM array needs to capture the PS ping in about 50 ms time window. The PS signal captured at the source receiver array was then time reversed and retransmitted backward to the vertical receiver array. A tight focus along the depth has been observed, which suggests that the VRA should be positioned around the PS with dense sampling. The focus has been computed for various ranges, viz., 0.5, 1 and 2 km. Re-focussing of TRM at ranges other than the PS range by an appropriate frequency shift has been investigated and the results are presented. The other results would include transmission loss at various ranges and for different bottom sound speed, field strength in range and depth and also results from investigations using a thinner TRM array with smaller number of elements. A comparison of results shows that keeping the aperture of the array is more important than the inter-element spacing given the number of transducers.

REFERENCES

[1] W. Kuperman, W. Hodgkiss, H. Song, T. Akal, C. Ferla, and D. Jackson, "Phase conjugation in the ocean: Experimental demonstration of an acoustic time reversal mirror," *J. Acoust. Soc. Am.* 103(1), pp. 25-40, 1998.

[2] W.S. Hodgkiss, H.C. Song, W.A. Kuperman, T. Akal, C. Ferla, D. Jackson, "A long range and variable focus phase conjugation experiment in shallow water," *J. Acoust. Soc. Am.* 105(3), pp. 1597-1604, 1999.

[3] H. Song, W. Hodgkiss, W. Kuperman, P. Roux, T. Akal, M. Stevenson, "Experimental demonstration of adaptive reverberation nulling using time reversal," *Acoust. Soc. Am.* 118, pp. 1381-1387, 2005.

[4] G. Edelmann, T. Akal, W.S. Hodgkiss, S. Kim, W. Kuperman, and H. Song, "An initial demonstration of underwater acoustic communication using time reversal," *IEEE J. Oceanic Eng.* 28, pp. 602-609, 2002.

[5] A. Baggeroer, W. Kuperman, and P. Mikhalevsky, "An overview of matched field methods in ocean acoustics," *IEEE J. Oceanic Eng.* 18, pp. 401-424, 1993.

[6] H. Song, W. Kuperman, and W.S. Hodgkiss, "A time reversal mirror with variable range shift," *J. Acoust. Soc. Am.* 103, pp. 3234-3240, 1998.

[7] W. Hodgkiss, W. Kuperman, H. Song, T. Akal, C. Ferla, and D. Jackson, "Time reversal focusing with less than a full water column source array," *J. Acoust. Soc. Am.* 102, pp. 3171, 1997.

[8] W. Hodgkiss, J. Skinner, G. Edmonds, R. Harris, and D. Ensberg, "A high frequency phase conjugation array," *IEEE Oceans 2001*, Hawaii, 2001.